

Blind modal identification of output-only non-proportionally-damped structures by time-frequency complex independent component analysis

Satish Nagarajaiah^{*1} and Yongchao Yang^{2a}

¹Department of Civil and Environmental Engineering and Department of Mechanical Engineering, Rice Univ., Houston, TX, USA

²Department of Civil and Environmental Engineering, Rice Univ., Houston, TX, USA

(Received January 25, 2014, Revised May 8, 2014, Accepted May 23, 2014)

Abstract. Recently, a new output-only modal identification method based on time-frequency independent component analysis (ICA) has been developed by the authors and shown to be useful for even highly-damped structures. In many cases, it is of interest to identify the complex modes of structures with non-proportional damping. This study extends the time-frequency ICA based method to a complex ICA formulation for output-only modal identification of non-proportionally-damped structures. The connection is established between complex ICA model and the complex-valued modal expansion with sparse time-frequency representation, thereby blindly separating the measured structural responses into the complex mode matrix and complex-valued modal responses. Numerical simulation on a non-proportionally-damped system, laboratory experiment on a highly-damped three-story frame, and a real-world highly-damped base-isolated structure identification example demonstrate the capability of the time-frequency complex ICA method for identification of structures with complex modes in a straightforward and efficient manner.

Keywords: output-only modal identification; complex modes; non-proportional damping; blind source separation; complex independent component analysis; time-frequency analysis

1. Introduction

Recently, a family of blind source separation (BSS) based output-only modal identification methods has been developed, providing an efficient alternative to perform non-parametric modal identification. It has been shown that modal information can be directly extracted by several BSS techniques, such as independent component analysis (ICA) (Kerschen *et al.* 2007, Yang and Nagarajaiah 2012, 2013), second order blind identification (SOBI) (Poncelet *et al.* 2007, McNeill and Zimmerman 2008, Hazra *et al.* 2010, Abazarsa *et al.* 2013, Antoni and Chuahan 2013), complexity pursuit (CP) (Yang and Nagarajaiah 2013b), and sparse component analysis (Yang and Nagarajaiah 2013c). One main advantage of the BSS based methods lie in its straightforward

*Corresponding author, Professor, E-mail: Satish.Nagarajaiah@rice.edu

^a Postdoctoral Research Associate, formerly Ph.D. student, E-mail: Yongchao.Yang@rice.edu

implementation: based on the implicit modal expansion of the structural responses, mode matrix and modal responses are directly separated by the BSS technique, without model assumption and parameter-fitting.

Most of the existing BSS based methods have been adopted to identify real-valued modes with the assumption of proportional damping of structures. In practice, identification of complex modes would be of interest in many cases, since real structures possess non-proportional damping, which cannot be neglected especially when coupled with high damping. While existing output-only methods for identification of complex modes, such as those based on Hilbert-Huang transform (Yang *et al.* 2003), wavelet transform (Erlicher and Argoul 2007), and blind modal identification (McNeill and Zimmerman 2008), have been shown to be effective in free vibration, other issues such as random vibration have not been fully addressed.

This study focuses on developing a new output-only complex mode identification method in the BSS framework. A time-frequency ICA method, short-time-Fourier-transform ICA (STFT-ICA), which is proposed by the authors for identification of proportionally highly-damped structures (Yang and Nagarajaiah 2013a), is further exploited to identify non-proportionally-damped structures. The established connection between the time-frequency ICA model and the modal expansion with sparse time-frequency representation, is naturally extended to the complex mode situations, thereby blindly separating the measured structural responses into the complex mode matrix and complex-valued modal responses. The numerical simulations on a non-proportionally-damped structure illustrate the ability of the short-time-Fourier-transform complex ICA (STFT-cICA) method in identifying complex modes in the presence of heavy noise and random excitation. A laboratory experiment study of a highly-damped structure and a real-world highly-damped base-isolated structure identification example are also presented for verification of the proposed STFT-cICA output-only modal identification method.

2. Time-frequency BSS based modal identification method

2.1 Modal expansion of complex modes

The governing equation of motion (EOM) of an n -DOF linear time-invariant system is

$$\mathbf{M}\ddot{\mathbf{x}}(t) + \mathbf{C}\dot{\mathbf{x}}(t) + \mathbf{K}\mathbf{x}(t) = \mathbf{f}(t) \quad (1)$$

where \mathbf{M} , \mathbf{C} , and \mathbf{K} are the constant mass, damping, and stiffness matrices (symmetric), respectively; $\mathbf{f}(t)$ is the external force vector applied to the system.

The system responses (displacements) $\mathbf{x}(t) = [x_1(t), x_2(t), \dots, x_n(t)]^T$ can be expressed by modal expansion as

$$\mathbf{x}(t) = \Phi \mathbf{q}(t) = \sum_{i=1}^n \boldsymbol{\phi}_i q_i(t) \quad (2)$$

then

$$\mathbf{q}(t) = \Phi^{-1} \mathbf{x}(t) \quad (3)$$

where $\mathbf{q}(t) = [q_1(t), q_2(t), \dots, q_n(t)]^T$ are the modal responses, and Φ is the mode matrix with ϕ_i as its i th column (mode shape) associated with the i th modal response $q_i(t)$.

In case of proportional damping, \mathbf{C} can be diagonalized by the normal mode matrix Φ_N and Eq. (1) can be decoupled by Φ_N ; $\Phi = \Phi_N$ and $\mathbf{q}(t)$ are both real-valued. When \mathbf{C} is non-proportional which can not be diagonalized by Φ_N ; however, Eq. (1) can still be decoupled by Φ in the state space and the modal expansion Eq. (2) still holds with both Φ and $\mathbf{q}(t)$ complex-valued (the details are shown in the appendix).

3. Theoretical background of BSS and ICA

The BSS technique (Hyvärinen and Oja 2000) is briefly reviewed in this section. The BSS problem usually assumes a linear instantaneous mixing model

$$\mathbf{x}(t) = \mathbf{A}\mathbf{s}(t) = \sum_{i=1}^n \mathbf{a}_i s_i(t) \quad (4)$$

where $\mathbf{x}(t) = [x_1(t), x_2(t), \dots, x_m(t)]^T$ and $\mathbf{s}(t) = [s_1(t), s_2(t), \dots, s_n(t)]^T$ are the observed mixture vector and the unknown source vector, and \mathbf{A} (full rank) is the constant mixing matrix needed to be estimated (\mathbf{a}_i denotes the i th column of \mathbf{A} associated with $s_i(t)$). It is assumed that $m = n$, i.e., \mathbf{A} is square. The over-determined BSS problem ($m > n$) can always be reduced to square BSS by principal component analysis (PCA), and the underdetermined BSS problem ($m < n$), where the number of mixture is insufficient, is beyond the scope of this study.

With only the observations $\mathbf{x}(t)$ known, Eq. (4) cannot be solved mathematically. ICA makes a general assumption that the sources are statistically independent at each instant t . It searches for a proper de-mixing matrix \mathbf{W} such that the components $\mathbf{y}(t) = [y_1(t), y_2(t), \dots, y_n(t)]^T$ recovered by

$$\mathbf{y}(t) = \mathbf{W}\mathbf{x}(t) \quad (5)$$

are as independent as possible and $\mathbf{W} = \mathbf{A}^{-1}$. Independence is measured by non-Gaussianity; specifically, the recovered $y_i(t)$ maximizes non-Gaussianity using some contrast function such as kurtosis and negentropy.

Although most studies address the real-valued ICA model, it can also be extended to complex-valued cases. For this study, the fast complex ICA method is used based on fix-point iteration which has excellent efficiency and consistency; the details of this algorithm can be found in (Bingham and Hyvärinen 2000).

3.1 STFT-cICA output-only modal identification method

Noting the similarity between Eqs. (2) and (4), Kerschen *et al.* (2007) proposed that the

time-domain modal responses can be viewed as sources provided that they have incommensurable frequencies among different modes, and Eq. (2) can be directly solved by ICA; however, it is only suitable for lightly-damped structures (only within 1%). While the ICA method based on the Hebbian-like algorithm overcomes this difficulty, it is incapable of handling random vibration (McNell 2007). Yang and Nagarajaiah (2013a) transformed the modal expansion to the sparse time-frequency domain to alleviate the damping effects, followed by the use of ICA; promising results were obtained even in the presence of heavy noise and random excitation.

The time-frequency ICA method can be readily extended for identification of complex modes. Taking STFT to both sides of Eq. (2) (complex-valued) yields a two-dimensional time-frequency BSS model as

$$\mathbf{X}(f, \tau) = \Phi \mathbf{Q}(f, \tau) = \sum_{i=1}^n \phi_i Q_i(f, \tau) \quad (6)$$

where

$$\mathbf{X}(f, \tau) = \frac{1}{\sqrt{2\pi}} \int_{-\infty}^{\infty} \mathbf{x}(t') h(t' - \tau) e^{-j2\pi f t'} dt' \quad (7)$$

$$\mathbf{Q}(f, \tau) = \frac{1}{\sqrt{2\pi}} \int_{-\infty}^{\infty} \mathbf{q}(t') h(t' - \tau) e^{-j2\pi f t'} dt' \quad (8)$$

in which f and τ are the frequency and window indices, respectively; $h(t)$ is some window function (e.g., the Hamming window). Note that instead of using only the absolute values of $\mathbf{X}(f, \tau)$ (and $\mathbf{Q}(f, \tau)$) in STFT-ICA (Yang and Nagarajaiah 2013a), both the real and imaginary (phase information) parts of $\mathbf{X}(f, \tau)$ are retained in Eq. (6).

Sequentially concatenating all the windowed STFTs and combining the window and frequency indices gives a one-dimensional *complex* BSS problem

$$\mathbf{X}_{f\tau} = \Phi \mathbf{Q}_{f\tau} \quad (9)$$

which can be solved by Fast complex ICA.

As introduced in STFT-ICA, the linear transform STFT ensures Eq. (9) retains the information of Eq. (2): the (complex) mixing mode matrix Φ remains invariant, and the $\mathbf{Q}_{f\tau}$ is independent with *disjoint* sparse time-frequency representation (in both real and imaginary axis), inheriting the incommensurable frequencies of $\mathbf{q}(t)$. Therefore, they can be directly extracted from the mixtures $\mathbf{X}_{f\tau}$ by complex ICA

$$\tilde{\mathbf{Q}}_{f\tau} = \tilde{\mathbf{W}} \mathbf{X}_{f\tau} \quad (10)$$

simultaneously yielding the estimated complex mode matrix $\tilde{\Phi} = \tilde{\mathbf{A}} = \tilde{\mathbf{W}}^{-1}$. Once $\tilde{\Phi}$ are estimated, the time-domain modal responses can be recovered using the de-mixing matrix according to Eq. (3) as

$$\tilde{\mathbf{q}}(t) = \tilde{\mathbf{W}} \mathbf{x}(t) \quad (11)$$

From the real part of which the modal frequencies and damping ratios (free vibration) are readily estimated by Fourier transform (FT) and logarithm decrement technique (LT) (Nagarajaiah, S and Basu 2009), respectively.

4. Numerical simulations

Numerical study is conducted to validate the proposed STFT-cICA modal identification method. For convenient comparison, the linear time-invariant lumped-mass-spring model (Fig. 1) with complex modes from (McNeill and Zimmerman 2008) is considered herein, whose EOM is

$$\mathbf{M} = \begin{bmatrix} 3 & 0 & 0 \\ 0 & 2 & 0 \\ 0 & 0 & 1 \end{bmatrix} \quad \mathbf{K} = \begin{bmatrix} 4 & -2 & 0 \\ -2 & 4 & -2 \\ 0 & -2 & 10 \end{bmatrix} \quad \mathbf{C} = \begin{bmatrix} 0.1856 & 0.2290 & -0.9702 \\ 0.2290 & 0.0308 & -0.0297 \\ -0.9702 & -0.0297 & 0.1241 \end{bmatrix}$$

Free vibration, noisy vibration, stationary random vibration, and non-stationary random vibration are studied, respectively. Newmark-Beta algorithm is used to obtain the time histories of the system responses (displacements) from the EOM, with a sampling frequency of 10 Hz.

The procedures of STFT-cICA output-only modal identification algorithm are as follows. System responses are first transformed by the STFT, where the Hamming window is used. The windowed STFTs are then sequentially concatenated and used as mixtures fed into the BSS model, which is subsequently solved by Fast complex ICA using the Gaussian contrast function. The obtained mixing matrix is the estimation of the complex mode matrix. Using Eq. (11), the de-mixing matrix is used to decouple the system responses into the modal responses. From the real part of the recovered time-domain modal responses, the frequencies and damping ratios can be computed using Fourier transform (power spectral density (PSD)) and logarithm decrement technique, respectively.

Since the mode shapes are complex-valued, they are first translated to equivalent real-valued using the standard method described in (McNeill and Zimmerman 2008) such that the correlation between the estimated mode shapes by STFT-cICA and the theoretical mode shapes can be measured by the modal assurance criterion (MAC), defined as

$$\text{MAC}(\tilde{\varphi}_i, \varphi_i) = \frac{(\tilde{\varphi}_i^T \cdot \varphi_i)^2}{(\tilde{\varphi}_i^T \cdot \tilde{\varphi}_i)(\varphi_i^T \cdot \varphi_i)} \quad (12)$$

ranging from 0 to 1, where 0 means no correlation and 1 means perfect correlation. $\tilde{\varphi}_i$ and φ_i denote the i th estimated and exact mode shapes, respectively.

4.1 Free vibration

The initial conditions of $\mathbf{x}(0) = [1 \ 0 \ 1]^T$ and $\dot{\mathbf{x}}(0) = [0 \ 0 \ 0]^T$ are set to induce free vibration of the system (Fig. 2). It is seen in Table 1 that the identified frequency and damping ratio match the analytical results well. The estimated mode matrix (the columns are in the original order of ICA estimation and not re-arranged by the order of mode number, although which can be easily done, see (Yang and Nagarajaiah 2013)'s discussion; for example, the 1st column is the first

ICA-estimated mode, but it corresponds to the 3rd mode by looking at the frequency of the corresponding estimated modal response) is

$$\tilde{\Phi} = \begin{bmatrix} 0.0091 + 0.1238j & 1.0000 & -0.6793 + 0.0359j \\ -0.1217 - 0.0148j & 0.9467 - 0.0182j & 1.0000 \\ 1.0000 & 0.2016 - 0.0941j & 0.2704 + 0.1333j \end{bmatrix}$$

which also matches the analytical mode matrix

$$\Phi = \begin{bmatrix} 1.0000 & -0.6778 & 0.0357j + 0.009 \\ 0.9447 & 0.0232j & 1.0000 - 0.122 \\ 0.2016 & 0.0955j & 0.2703 & 0.1330j \end{bmatrix}$$

with high MAC values and small errors (in an 2-norm measure) shown in Table 2 (noise-free case). For illustration, the real-part of the recovered modal responses is presented in Fig. 3. As can be seen, the system responses containing multiple frequencies (their power spectral density (PSD) are separated well by the STFT-cICA method, yielding the mono-component modal responses, which are exponentially decaying sinusoids. It is also seen that STFT-cICA has comparable accuracy to blind modal identification (BMID) (McNeill and Zimmerman 2008), while using straightforward implementation (directly yielding complex modes)

4.2 Noisy vibration & random vibration

It has been shown in (Yang and Nagarajaiah 2013a) that STFT-ICA holds well in the presence of noise and random excitation; this section investigates whether if such is true for STFT-cICA.

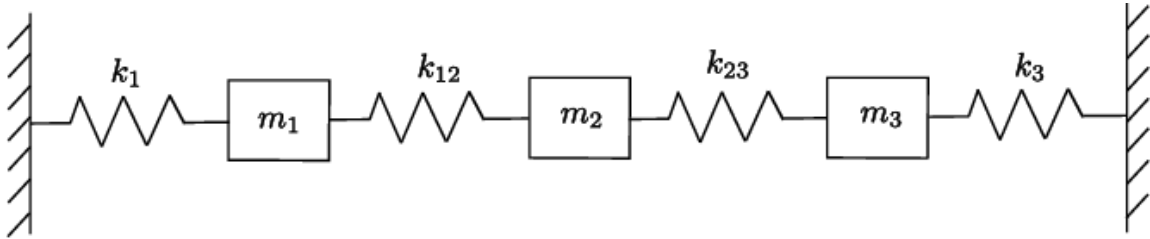


Fig. 1 The mass-spring non-proportionally-damped model for numerical simulations

Table 1 Identified results by STFT-cICA in free vibration without noise

Mode	Frequency (Hz)			Damping Ratio (%)		
	Analytical	BMID	STFT-cICA	Analytical	BMID	STFT-cICA
1	0.136	0.136	0.137	3.02	2.93	3.08
2	0.247	0.247	0.244	1.37	1.36	1.38
3	0.500	0.500	0.498	1.71	1.69	1.78

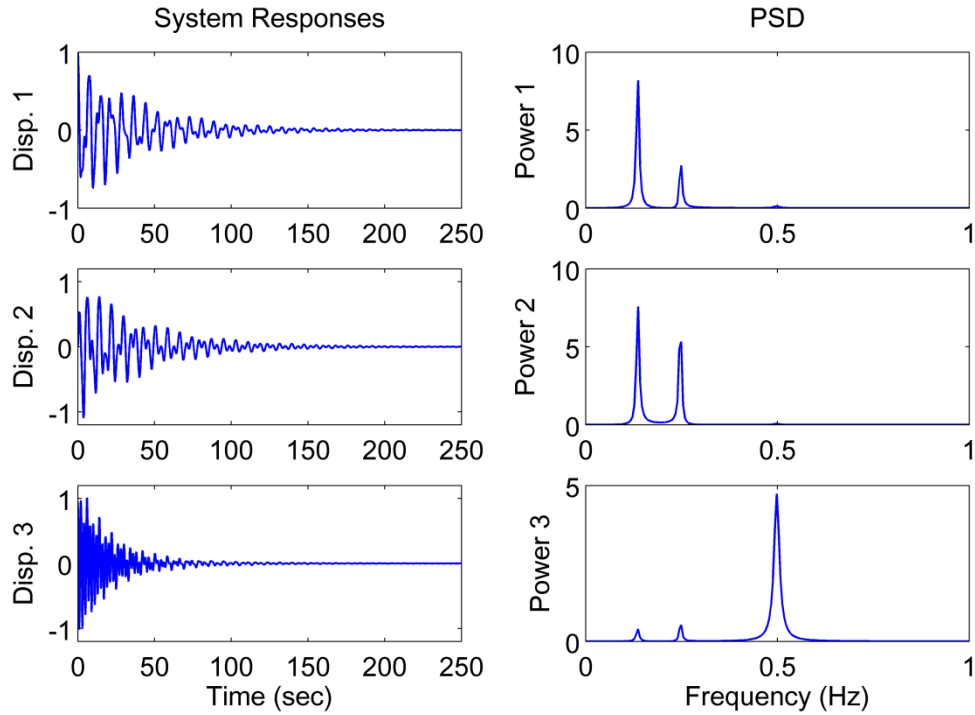


Fig. 2 Free vibration system responses of the numerical model (with complex modes)

Table 2 MAC values and norm-2 errors between STFT-cICA identified mode shapes and analytical ones

Mode	Free		SNR=10 dB		Stationary		Non-stationary	
	Error	MAC	Error	MAC	Error	MAC	Error	MAC
1	0.0057	1.0000	0.0138	1.0000	0.0445	0.9999	0.0063	1.0000
2	0.0020	1.0000	0.0244	0.9998	0.0491	0.9998	0.0061	1.0000
3	0.00005	1.0000	0.0242	0.9995	0.0081	1.0000	0.0008	1.0000

Table 3 MAC values between STFT-cICA and ERA of the experimental structure, compared to those between STFT-ICA and ERA

Mode	STFT-ICA	STFT-cICA
1	0.99	0.99
2	0.69	0.97
3	0.91	0.95

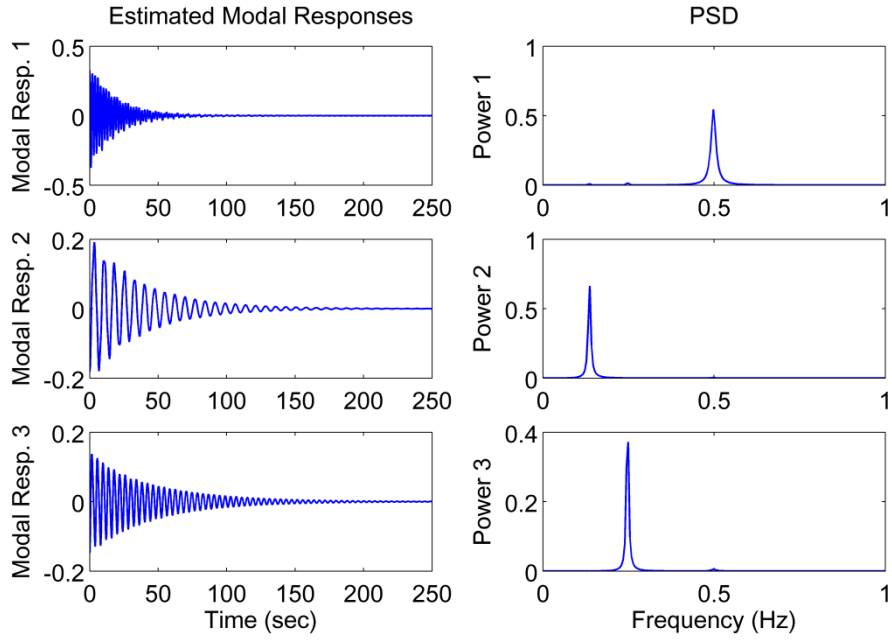


Fig. 3 The recovered modal responses (real part) by STFT-cICA

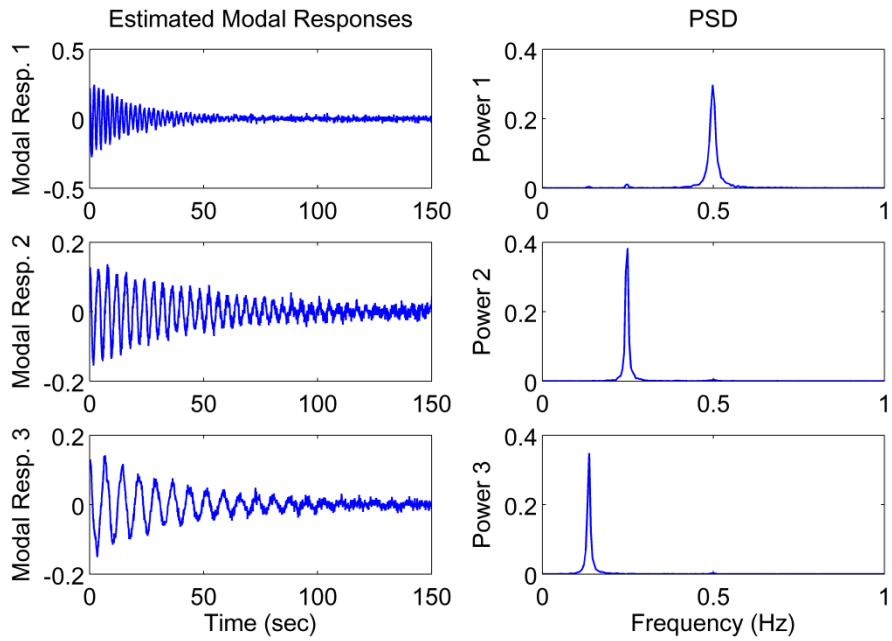


Fig. 4 The recovered modal responses (real part) by STFT-cICA from noisy system responses (SNR=10 dB)

Zero-mean Gaussian white noise (GWN) with a signal-to-noise-ratio (SNR) of 10 dB (root-mean-square noise level of 31.6%) is added to contaminate the free vibration system responses. It is seen that the MAC values (SNR=10 dB case in Table 2) are still close to perfect correlation and the errors are small, indicating the estimated complex mode shapes are accurate. The recovered modal responses (real-part) are shown in Fig. 4, from which the frequency and damping ratio can still be estimated accurately.

Random vibration is also considered. Stationary GWN, as well as non-stationary white noise (WN) modeled by modulating the GWN with an exponential decaying function, are used to excite the system, respectively. Similar accuracy can also be seen from Figs. 5 and 6 and Table 2. As evident, STFT-cICA performs well in the presence of noise and random excitation; as explained in (Yang and Nagarajaiah 2013a) for STFT-ICA, it is because of its ability of accurately separating the sparse time-frequency representations of the monotone modal responses, as long as which are dominant in the time-frequency domain even in the presence of heavy noise and random vibration.

5. Experimental verification

STFT-cICA is also conducted to identify the complex modes of a highly-damped three-story steel frame, which has been previously described in (Yang and Nagarajaiah 2013a). As shown in Fig. 7, an extra damper is present between the base and the first floor. Free vibration is induced by a horizontal impact at the top floor (the third mass), and the responses from three accelerometers are recorded with a sampling frequency of 5128 Hz.

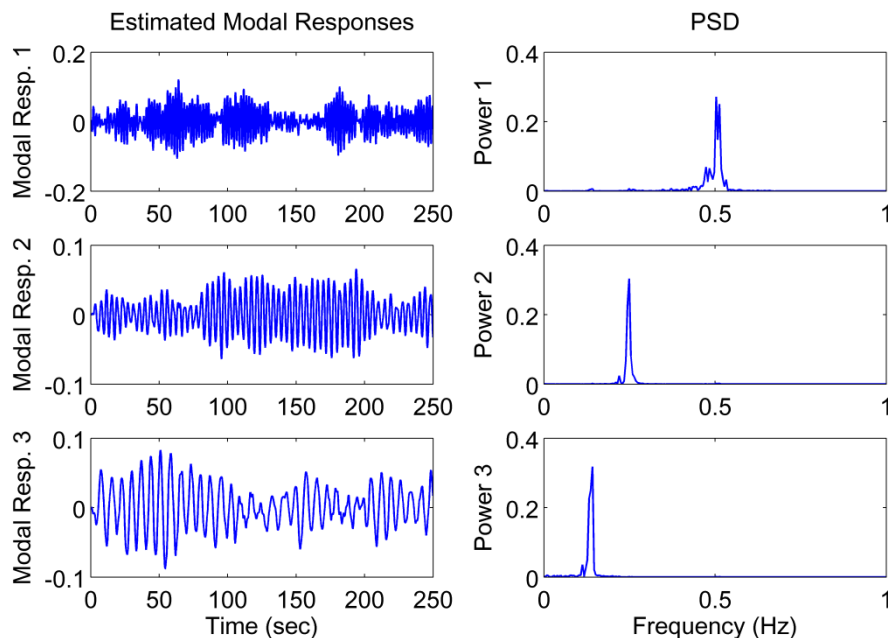


Fig. 5 The recovered modal responses (real part) by STFT-cICA from system responses of random vibration (with stationary Gaussian white noise excitation)

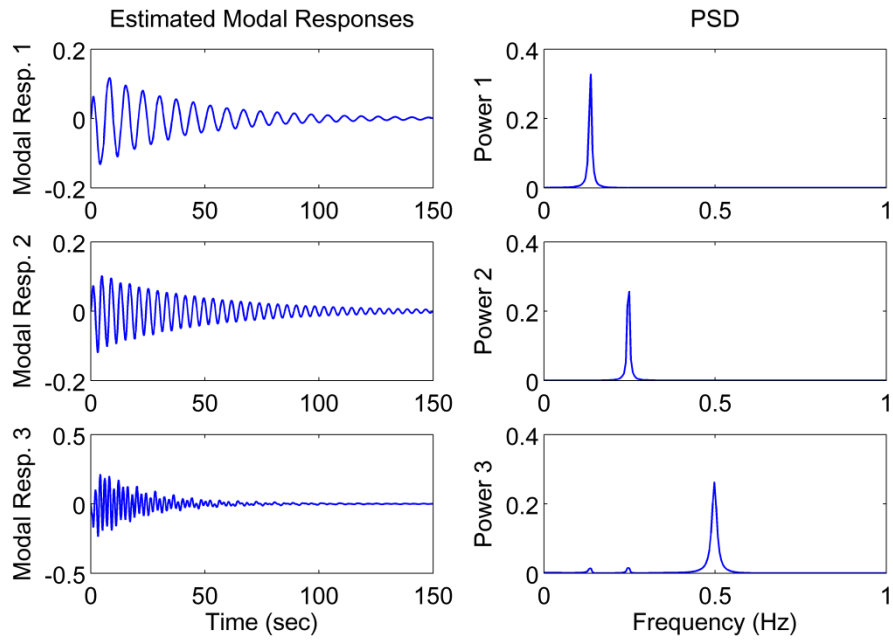


Fig. 6 The recovered modal responses (real part) by STFT-cICA from system responses of random vibration (with non-stationary constant exponentially-decaying Gaussian white noise excitation)

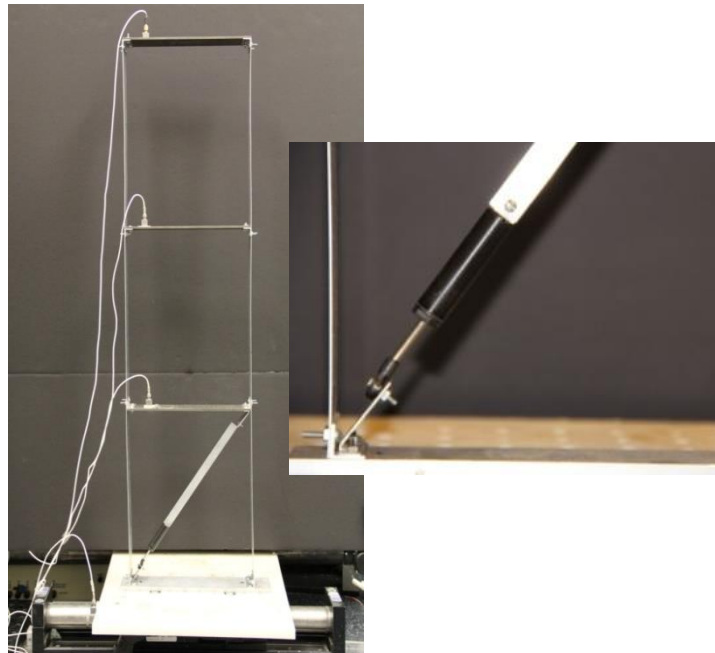


Fig. 7 The experimental three-story steel frame with an extra fluid damper embedded between the base and the first floor

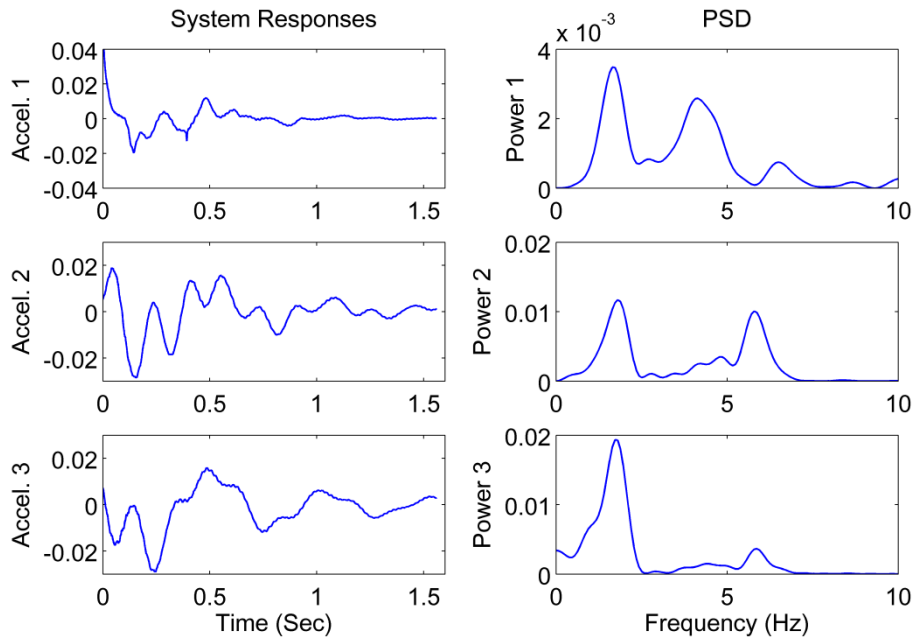


Fig. 8 Free vibration system responses of the experimental structure

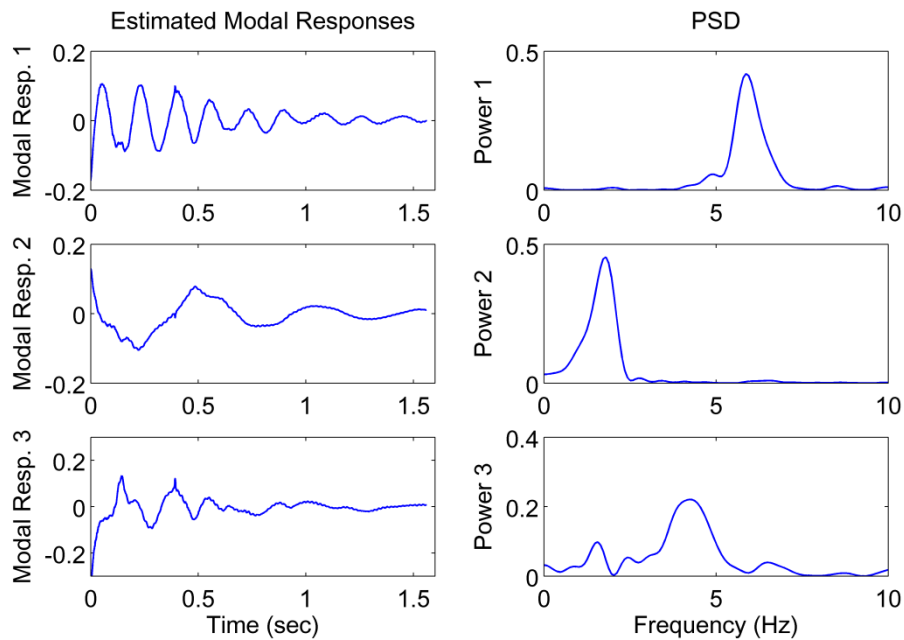


Fig. 9 The recovered modal responses (real part) by STFT-cICA of the experimental structure

STFT-cICA is applied on the short-duration data set (due to high damping as in (Yang and Nagarajaiah 2013a)), without other preprocessing, and the system responses and the recovered modal responses (real-part) are shown in Figs. 8 and 9, showing that the coupled structural responses are separated into monotone modal responses. The results obtained by the ERA method conducted on the same data set are used for reference for calculation of the MAC values. Table 3 shows that the mode shapes estimated by STFT-cICA has a high correlation (higher MAC values) with those by eigensystem realization algorithm (ERA) (Juang and Pappa 1985), indicating that the non-parametric STFT-cICA has a comparable accuracy with the parametric ERA. The higher MAC of STFT-cICA than that of STFT-ICA also indicates that it would be more useful to identify the complex modes of highly-damped structure. The frequency and damping ratio identified by STFT-cICA is very close to those by STFT-ICA (Yang and Nagarajaiah 2013a) and ERA, but they are not presented here for conciseness. The reason for a slight mixture of the first mode into the identified second mode (the bottom plot in the right side of Fig. 9) was discussed in the authors' previous work and is not repeated here.

6. Identification of seismically excited real-world structure

The proposed STFT-cICA method is applied to identify the highly-damped base-isolated USC hospital building (Fig. 10) using its recorded seismic responses during the 1994 Northridge earthquake (Nagarajaiah and Sun 2000, Nagarajaiah and Dharap 2003). STFT-cICA is applied on the same set of seismic responses (Fig. 11, see Yang and Nagarajaiah 2013a, Nagarajaiah and Sun 2000) for detailed description of this structure and the used data set) of this structure and the identification results are shown in Fig. 12 and Table 4, where the MAC values are computed between the normal modes by analytical model and the complex modeshapes (converted to real-valued modes) estimated by STFT-cICA.

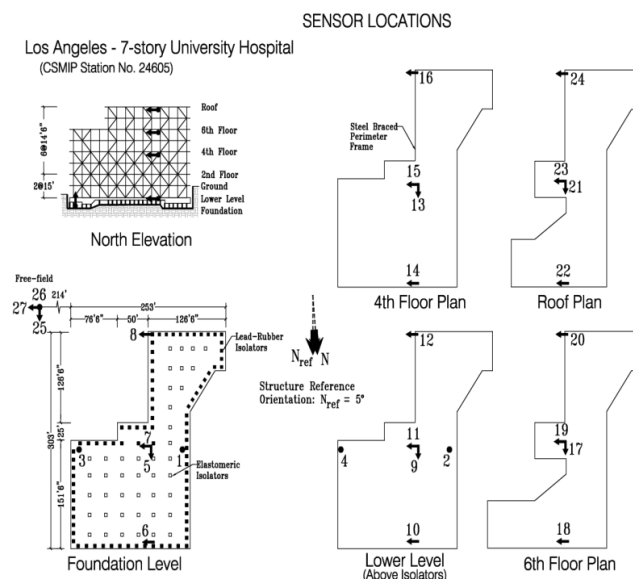


Fig. 10 The USC hospital building and its sensor outline

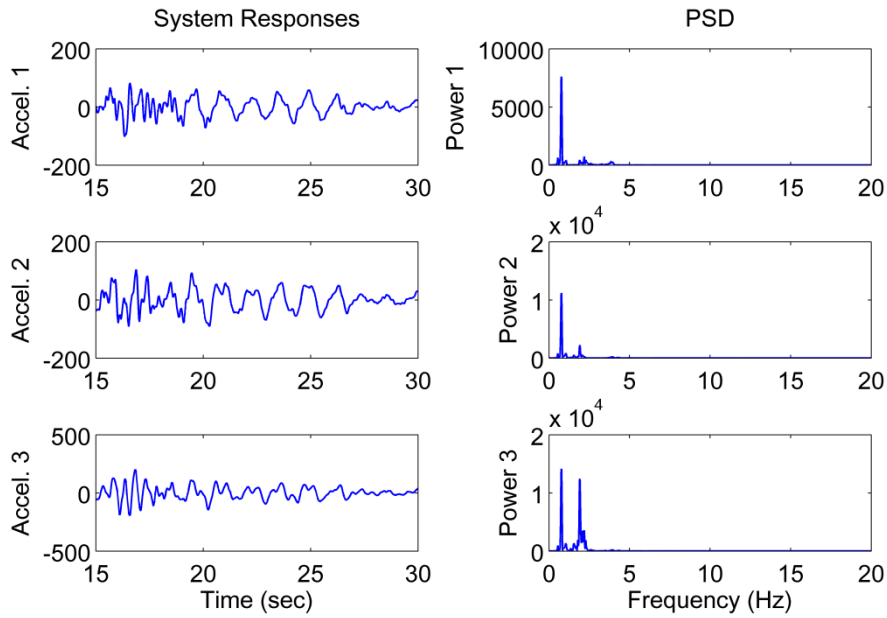


Fig. 11 Recorded seismic responses of the USC hospital building during 1994 Northridge Earthquake

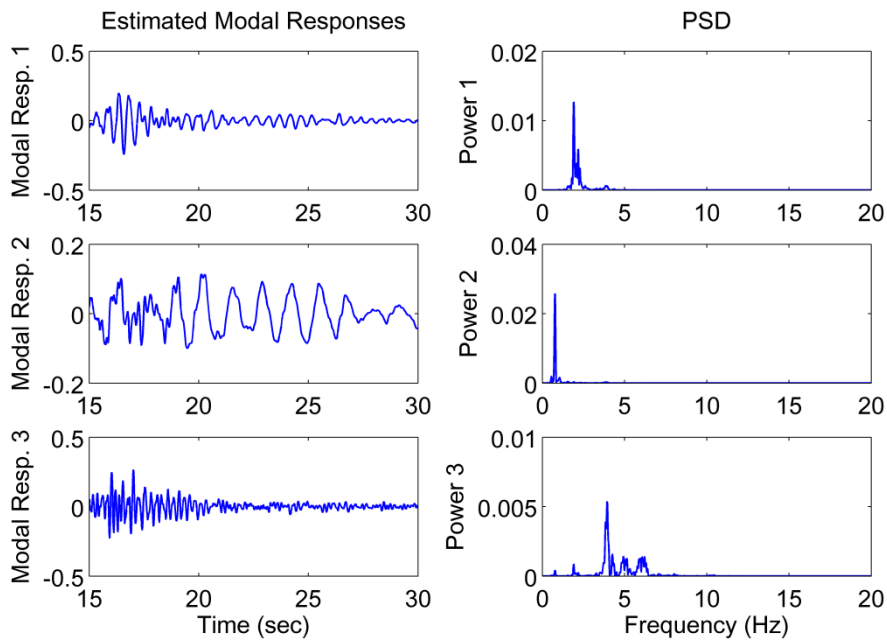


Fig. 12 The recovered modal responses (real part) by STFT-cICA of the USC hospital building

Table 4 MAC values between STFT-cICA and the analytical model of the USC hospital building, compared to those between STFT-ICA and the analytical model

Mode	STFT-ICA	STFT-cICA
1	0.98	0.99
2	0.93	0.97
3	0.30	0.48

Fig. 12 shows that the structural responses are successfully separated into monotone modal responses. Table 4 shows the MAC values of the modes, illustrating that the identified modes yield reasonable agreement with those of the analytical model, including the weakly-excited third mode with reasonable improvement over that by STFT-ICA, although those of the first two modes show slight degradation.

7. Conclusions

This study extends the previously proposed time-frequency ICA output-only modal identification method to identify complex modes of non-proportionally-damped structures. The similarity between the time-frequency ICA model and the modal expansion with sparse time-frequency representation is further exploited in the complex-valued situation, through which the complex-valued mode matrix and modal responses can be directly extracted by the time frequency complex ICA (STFT-cICA).

Numerical simulations are conducted on a non-proportionally-damped structure and laboratory experiments on a highly-damped three-story frame. Results show that the time-frequency complex ICA method is able to accurately identify the complex modes. It is expected to be a straightforward and efficient (with Fast complex ICA algorithm) alternative to identify output-only practical structures (especially highly-damped) with significant non-proportional damping.

References

- Abazarsa, F., Ghahari, S.F., Nateghi, F. and Taciroglu, E. (2013), "Response-only modal identification of structures using limited sensors", *Struct. Control Health Monit.*, **20**(6), 987-1006.
- Antoni, J. and Chuahan S.A (2013), "Study and extension of second-order blind source separation to operational modal analysis", *J. Sound Vib.*, **332**(4), 1079-1106.
- Bingham, E. and Hyvärinen, A. (2000), "A fast fixed-point algorithm for independent component analysis of complex valued signals", *Int. J. Neural Syst.*, **10**(1), 1-8.
- Erlicher, S. and Argoul, P. (2007), "Modal identification of linear non-proportionally damped systems by wavelet transform", *Mech. Syst. Signal Pr.*, **21**(3), 1386-1421.
- Hazra, B., Roffel, A.J., Narasimhan, S. and Pandey, M.D. (2010), "Modified cross-correlation method for the blind identification of structures", *J. Eng. Mech. -ASCE*, **136**(7), 889-897.
- Hyvärinen, A. and Oja, E. (2000), "Independent component analysis: algorithms and applications", *Neural Networks*, **13**(4-5), 411-430.

- Juang, J.N. and Pappa, R.S. (1985), "An eigen system realization algorithm for modal parameter identification and model reduction", *J. Guid. Control Dynam.*, **8**(5), 620-627.
- Kerschen, G., Poncelet, F. and Golinval, J.C. (2007), "Physical interpretation of independent component analysis in structural dynamics", *Mech. Syst. Signal Pr.*, **21**(4), 1561-1575.
- McNeill, S. (2007), *Modal identification using blind source separation techniques*, Ph.D. dissertation, The Department of Mechanical Engineering, University of Houston.
- McNeill, S.I. and Zimmerman, D.C. (2008), "A framework for blind identification using joint approximate diagonalization", *Mech. Syst. Signal Pr.*, **22**(7), 1526-1548.
- Nagarajaiah, S. and Basu, B. (2009), "Output only identification and structural damage detection using time frequency and wavelet techniques", *Earthq. Eng. Eng. Vib.*, **8**(4), 583-605.
- Nagarajaiah, S. and Dharap, P. (2003), "Reduced order observer based identification of base isolated buildings", *Earthq. Eng. Eng. Vib.*, **2**(2), 237-244.
- Nagarajaiah, S. and Sun, X. (2000), "Response of base-isolated USC hospital building in Northridge earthquake", *J. Struct. Eng. - ASCE*, **126**(10), 1177-1186.
- Poncelet, F., Kerschen, G., Golinval, J.C. and Verhelst, D. (2007), "Output-only modal analysis using blind source separation techniques", *Mech. Syst. Signal Pr.*, **21**(6), 2335-2358.
- Yang, J.N., Lei, Y., Pan, S. and Huang, N. (2003), "System identification of linear structures based on Hilbert-Huang spectral analysis, part 2: complex modes", *Earthq. Eng. Struct. D.*, **32**(10), 1533-1554.
- Yang, Y. and Nagarajaiah S. (2012), "Blind identification of damage in time-varying system using independent component analysis with wavelet transform", *Mech. Syst. Signal Pr.*, **47**(1-2), 3-20.
- Yang, Y and Nagarajaiah, S. (2013a), "Time-frequency blind source separation using independent component analysis for output-only modal identification of highly-damped structures", *J. Struct. Eng. - ASCE*, **139**(10), 1780-1793.
- Yang, Y. and Nagarajaiah, S. (2013b), "Blind modal identification of output-only structures in time domain based on complexity pursuit", *Earthq. Eng. Struct. D.*, **42**(13), 1885-1905.
- Yang, Y. and Nagarajaiah, S. (2013c), "Output-only modal identification with limited sensors using sparse component analysis", *J. Sound Vib.*, **332**(19), 4741-4765.

Appendix

Eq. (1) can be represented in the state space (making t implicit)

$$\mathbf{B}\dot{\mathbf{z}} + \mathbf{T}\mathbf{z} = \mathbf{g} \quad (13)$$

where

$$\mathbf{z} = \begin{Bmatrix} \mathbf{x} \\ \dot{\mathbf{x}} \end{Bmatrix} \quad \mathbf{B} = \begin{bmatrix} \mathbf{C} & \mathbf{M} \\ \mathbf{M} & \mathbf{0} \end{bmatrix} \quad \mathbf{T} = \begin{bmatrix} \mathbf{K} & \mathbf{0} \\ \mathbf{0} & -\mathbf{M} \end{bmatrix} \quad \mathbf{g} = \begin{Bmatrix} \mathbf{f} \\ \mathbf{0} \end{Bmatrix}$$

The $2n \times 2n$ system matrix is obtained by

$$\mathbf{V} = -\mathbf{B}^{-1}\mathbf{T} = \begin{bmatrix} \mathbf{0} & \mathbf{I} \\ -\mathbf{M}^{-1}\mathbf{K} & -\mathbf{M}^{-1}\mathbf{C} \end{bmatrix} \quad (14)$$

with n pairs of complex conjugate eigenvalues λ_i and $2n$ -dimensional eigenvectors \mathbf{u}_i

$$\mathbf{\Lambda} = \text{diag}[\lambda_1 \quad \lambda_2 \quad \cdots \quad \lambda_n \quad \lambda_1^* \quad \lambda_2^* \quad \cdots \quad \lambda_n^*]$$

$$\mathbf{U} = [\mathbf{u}_1 \quad \mathbf{u}_2 \quad \cdots \quad \mathbf{u}_n \quad \mathbf{u}_1^* \quad \mathbf{u}_2^* \quad \cdots \quad \mathbf{u}_n^*]$$

The state space system responses \mathbf{z} can then be expressed by

$$\mathbf{z}(t) = \mathbf{U}\mathbf{p}(t) = \sum_{i=1}^{2n} \mathbf{u}_i p_i(t) \quad (15)$$

where $\mathbf{p}(t) = [\mathbf{q}(t) \quad \mathbf{q}^*(t)]^T$ (complex-valued). Only expressing $\mathbf{x}(t)$ gives

$$\mathbf{x}(t) = \bar{\mathbf{U}}\mathbf{q}(t) = \sum_{i=1}^n \bar{\mathbf{u}}_i q_i(t) + \sum_{i=1}^n \bar{\mathbf{u}}_i^* q_i^*(t) \quad (16)$$

The ‘bar’ symbol denotes the upper n rows of the $2n$ dimension. Explicitly expressing the complex $\mathbf{u}_i = \mathbf{u}_i^R + j\mathbf{u}_i^I$ (\mathbf{u}_i^R and \mathbf{u}_i^I are real-valued) and $q_i(t) = q_i^R(t) + j q_i^I(t) = e^{-\zeta_i \omega_{ni} t} (\alpha_i \cos \omega_i t + j \beta_i \sin \omega_i t)$ with real and imaginary parts and substituting to Eq. (16), one obtains

$$\mathbf{x}(t) = \sum_{i=1}^n (\mathbf{u}_i^R 2\alpha_i e^{-\zeta_i \omega_{ni} t} \cos \omega_i t - \mathbf{u}_i^I 2\beta_i e^{-\zeta_i \omega_{ni} t} \sin \omega_i t) \quad (17)$$

where ζ_i , ω_{ni} , and $\omega_i = \omega_{ni} \sqrt{1 - \zeta_i^2}$ are the i th damping ratio, natural frequency, damped frequency, respectively; α_i and β_i are constant determined by initial or forced conditions.

Supposing there is a valid expression

$$\mathbf{x}(t) = \sum_{i=1}^n \boldsymbol{\varphi}_i q_i'(t) \quad (18)$$

Also expressing $\boldsymbol{\varphi}_i = \boldsymbol{\varphi}_i^R + \mathbf{j}\boldsymbol{\varphi}_i^I$ ($\boldsymbol{\varphi}_i^R$ and $\boldsymbol{\varphi}_i^I$ are real-valued) and $q_i'(t) = q_i'^R(t) + \mathbf{j}q_i'^I(t) = e^{-\zeta_i \omega_i t} (\alpha_i' \cos \omega_i t + \mathbf{j}\beta_i' \sin \omega_i t)$ and substituting to Eq. (18) gives

$$\mathbf{x}(t) = \sum_{i=1}^n [(\boldsymbol{\varphi}_i^R + \mathbf{j}\boldsymbol{\varphi}_i^I)\alpha_i' e^{-\zeta_i \omega_i t} \cos \omega_i t + \mathbf{j}(\boldsymbol{\varphi}_i^R + \mathbf{j}\boldsymbol{\varphi}_i^I)\beta_i' e^{-\zeta_i \omega_i t} \sin \omega_i t] \quad (19)$$

Because the solution of the physical system $\mathbf{x}(t)$ is real, there exist the combinations $\mathbf{v}_{i1}c_{i1} = (\boldsymbol{\varphi}_i^R + \mathbf{j}\boldsymbol{\varphi}_i^I)\alpha_i'$ and $\mathbf{v}_{i2}c_{i2} = (\boldsymbol{\varphi}_i^R + \mathbf{j}\boldsymbol{\varphi}_i^I)\beta_i'$ are both real numbers, that is

$$\mathbf{x}(t) = \sum_{i=1}^n (\mathbf{v}_{i1}c_{i1} e^{-\zeta_i \omega_i t} \cos \omega_i t + \mathbf{v}_{i2}c_{i2} e^{-\zeta_i \omega_i t} \sin \omega_i t) \quad (20)$$

Obviously, Eqs. (17) and (20) are equivalent. This shows that the modal expansion Eq. (2) or Eq. (18) is valid for complex mode case.